BURIED-OBJECT DETECTION USING FREE-SPACE TIME-DOMAIN NEAR-FIELD MEASUREMENTS

S. Biju Kumar,[1] C. K. Aanandan,[1] and K. T. Mathew[1]
[1] Department of Electronics
Cochin University of Science and Technology
Cochin-682 022, Kerala, India

ABSTRACT: *The detection of buried objects using time-domain free-space measurements was carried out in the near field. The location of a hidden object was determined from an analysis of the reflected signal. This method can be extended to detect any number of objects. Measurements were carried out in the X- and Ku-bands using ordinary rectangular pyramidal horn antennas of gain ~ 15 dB. The same antenna was used as the transmitter and receiver. The experimental results were compared with simulated results by applying the two-dimensional finite-difference time-domain (FDTD) method, and agree well with each other. The dispersive nature of the dielectric medium was considered for the simulation.* © 2001 John Wiley & Sons, Inc. Microwave Opt Technol Lett 31: 45–47, 2001.

1. INTRODUCTION

One of the major hurdles for the peacekeepers of war is the extensive use of the most dangerous land mines planted by foes. Extensive research has been ongoing in land-mine detection. A mine with a nonmetallic covering makes it impossible for conventional metal detectors to detect it, so there is a need to develop new techniques for land-mine detection, which should be very effective in detecting mines even with low loss and low-contrast dielectric materials. Many researchers have concentrated their attention in this field. Montoya and Smith [1] detected land mines using resistively loaded vee dipoles. Demarest, Plumb, and Huang [2] calculated the fields scattered by buried objects when the sources are close enough to the air–ground interface. A novel method of detecting buried objects like underground pipes, voids, cables, etc., using ordinary pyramidal horns both in the *X*- and *Ku*-bands is presented by the authors.

2. THEORETICAL ANALYSIS

Theoretical work was carried out on the system as shown in Figure 1. The dielectric medium ($\varepsilon_s = 2.5$) is assumed to be dispersive, linear, homogeneous, and isotropic. The discretized Maxwell's expressions for space and time were given by Yee [3]. Incorporating the dispersive nature of the dielectric medium [4] in the constitutive FDTD equations, the expression for the *H*-field is kept unchanged as the medium is assumed to be nonmagnetic, and is given by

$$H_x(i, j, t + 1) = H_x(i, j, t)$$
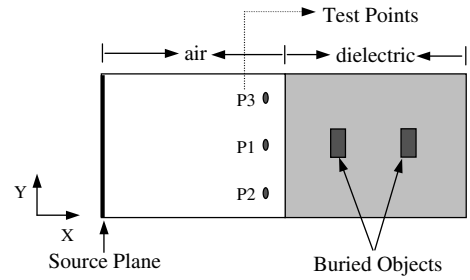$$- \frac{dt}{\mu_0 dy}(E_z(i, j, t) - E_z(i, j - 1, t)) \quad (1)$$

Figure 1 Schematic diagram of the theoretical system

$$H_y(i, j, t + 1) = H_y(i, j, t)$$
$$+ \frac{dt}{\mu_0 dx}(E_z(i, j, t) - E_z(i - 1, j, t)). \quad (2)$$

Because of the dispersive nature of the dielectric medium, the electric field is modified. The expression for the *E*-field is given by

$$E_z(i, j, t + 1)$$
$$= \frac{\varepsilon_\infty}{\varepsilon_\infty + \chi_0(i, j)} E_z(i, j, t)$$
$$+ \frac{1}{\varepsilon_\infty + \chi_0(i, j)} \sum_{m=0}^{t-1} E_z(i, j, t - m) \Delta \chi_m(i, j)$$
$$+ \frac{dt}{(\varepsilon_\infty + \chi_0(i, j))\varepsilon_0 dx}(H_y(i + 1, j, t) - H_y(i, j, t))$$
$$- \frac{dt}{(\varepsilon_\infty + \chi_0(i, j))\varepsilon_0 dy}(H_x(i, j + 1, t) - H_x(i, j, t))$$
$$(3)$$

where $\chi_0(i, j) = (\varepsilon_s - \varepsilon_\infty)(1 - \exp(-dt/t_0))$ is the susceptibility function, $\Delta \chi_m(i, j) = (\varepsilon_s - \varepsilon_\infty) \exp(-mdt/t_0)(1 - \exp(-dt/t_0))^2$, ε_s is the static permittivity of the dielectric, ε_∞ is the optical permittivity of the dielectric, t_0 is the relaxation time of the dielectric, and μ_0 is the permeability of free space.

A Gaussian pulse with $dt = 16.667$ ps, $T_0 = 41.667$ ps was executed at the source plane. A Yee cell was constructed from 140 grids in the *X*-direction and 80 grids in the *Y*-direction with a grid spacing $dx = 0.5$ cm and $dy = 0.5$ cm, respectively. Mur's boundary conditions [5] were applied at the boundaries. A dielectric object ($\varepsilon_s = 4$) of dimensions 3 cm $\times$ 3 cm was placed at a distance of 8 cm from the air–dielectric interface, as shown in figure 1. The response of the Gaussian pulse with time was noted. The same procedure was repeated with one more object placed at a distance of 18 cm away from the front surface, in line with the first object.

*P*1, *P*2, and *P*3 were three test points selected for study. The time-domain response from these points gives information on the buried object. This is explicit from Figure 2(a), (b). Figure 2(a) is the response obtained with a single object buried in the vessel, and Figure 2(b) is that when two objects are in a line. The dotted line represents the response at point *P*1, and the solid line that at *P*2 and *P*3. Peak *R*1 corresponds to the forward-moving Gaussian pulse, and *R*2 the
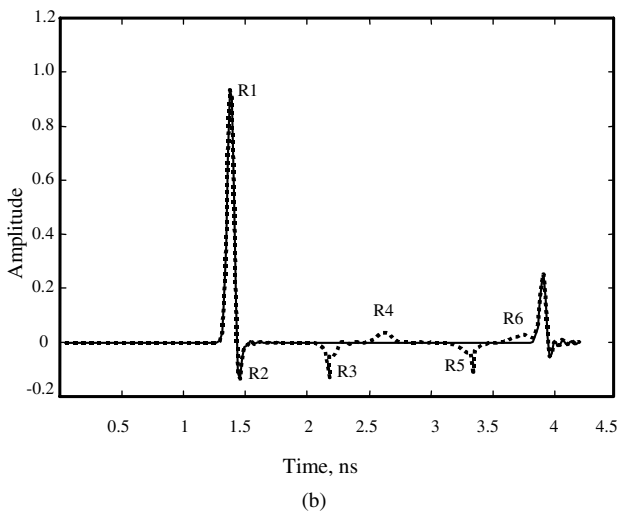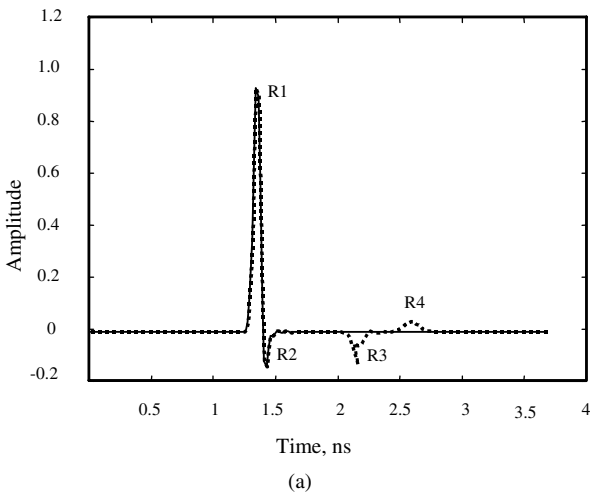
Figure 2 Theoretical time-domain responses. (a) With one buried object. (b) With two buried objects in line. ------ response at test point $P1$, —— response at points $P2$ and $P3$

reflection from the air–dielectric interface. $R3$ represents the reflection from the first buried object, and $R5$ that from the second object. $R4$ and $R6$ are the signals obtained due to the smaller dimensions of the objects. This can be avoided if the sample dimension is greater than the width of the Gaussian pulse. In Figure 2(b), the response after peak $R6$ is the repetition of the reflections.
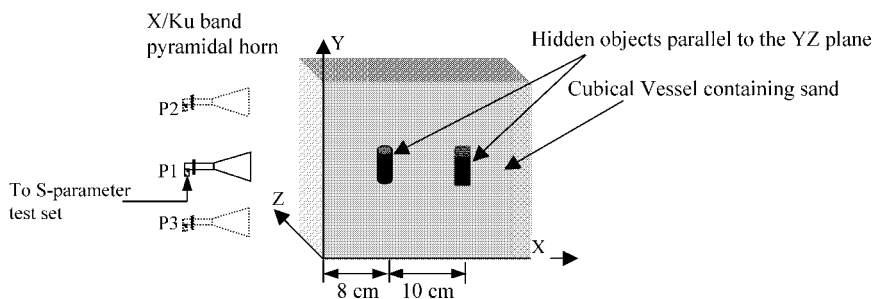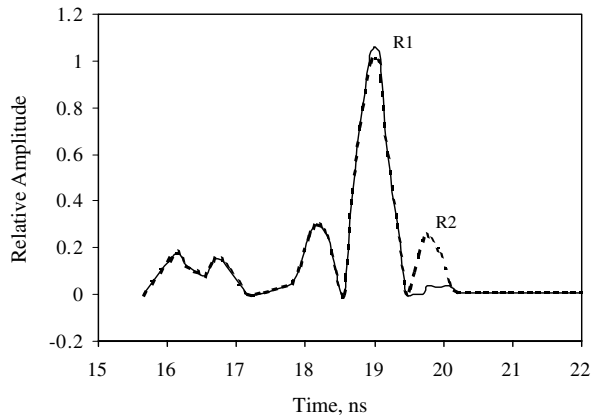
3. EXPERIMENTAL SETUP AND RESULTS

Experiments were performed in the X- and Ku-bands. A cubical vessel of dimensions 40 cm × 40 cm × 35 cm was filled with dry sand ($\varepsilon_s = 2.5$). The pyramidal horn antenna which was connected to one port of the S-parameter test set transmitted 10 mW power, and the same antenna received the reflected power from the vessel. The X-band horn antenna has a half-power beamwidth (HPBW) of 18° (E-plane) and 15.5° (H-plane) and aperture dimensions 9.8 cm × 7.5 cm. The respective values for the Ku-band horn antenna are 20°, 17°, and 5.7 cm × 4.4 cm. Both of the antennas have a gain of ∼ 15 dB. A dielectric block ($\varepsilon_r = 4$) of dimensions 7 cm × 3 cm × 3 cm was buried at a distance of 8 cm from the front surface of the vessel. Then the pyramidal horn antenna was set at each position $P1$, $P2$, and $P3$ (near-field points), as shown in Figure 3. The time-domain response was plotted with an HP 8510 C vector network analyzer. The same procedure was repeated, with one more object buried at a distance of 10 cm behind the first object. The results obtained are shown in Figure 4.

Figure 4(a), (b) represents the response obtained for single object in the X- and Ku-bands, respectively, and Figure 4(c) gives the response of two objects in the Ku-band. In the figures, $R1$ is the reflection from the front surface of the vessel. $R2$ corresponds to the reflection from the first object, and $R3$ that from the second object. The dotted line represents the time-domain response of the Gaussian pulse corresponding to point $P1$, and the solid lines corresponding to $P2$ and $P3$. The minor peaks appearing in front of $R1$ may be due to the discontinuities in the cables and connectors. A comparison of the theoretical and experimental results is shown in Table 1.

4. CONCLUSION

A simple and accurate method of detecting buried objects in the time domain has been presented. The results are compared with FDTD simulation results. An ordinary pyramidal horn with moderate aperture and nominal gain is used for the measurement. This technique finds wide applications in the detection of buried objects like land mines, pipes, voids, etc. The work can be extended to determine the dielectric parameters of hidden objects.
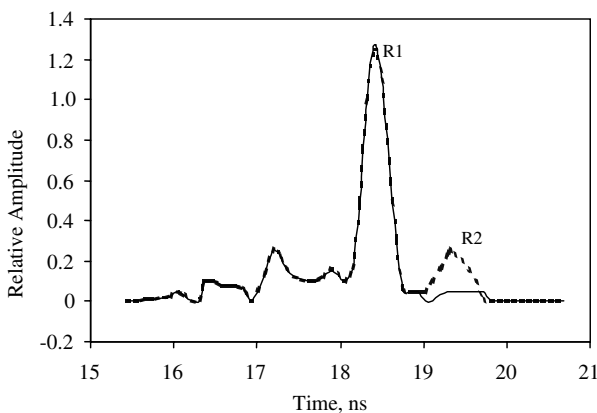
Figure 3 Experimental setup

TABLE 1   Comparison of Results from Theory and Experiment

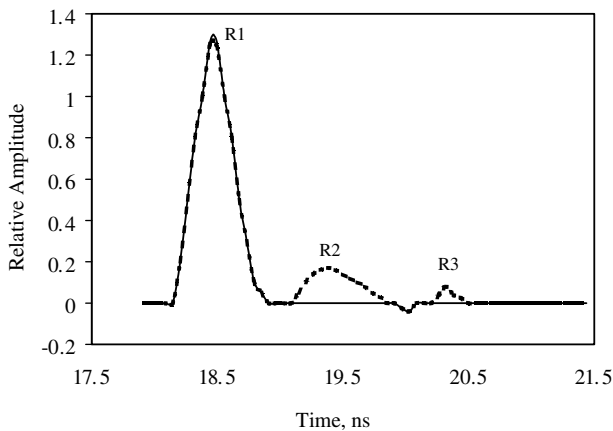| Actual Depth	Theoretical Results (from Fig. 2)	Experimental Results (from Fig. 3)
8 cm (first object)	$(R2-R3)/2 \rightarrow 0.3705$ ns (7.125 cm)[a]	$(R1-R2)/2 \rightarrow 0.4117$ ns, 0.465 ns (8.42 cm)(average)[a]
18 cm (second object)	$(R2-R5)/2 \rightarrow 0.92855$ ns (17.86 cm)[a]	$(R1-R3)/2 \rightarrow 0.9254$ ns (17.79 cm)[a]

[a] The velocity factor in the dielectric is incorporated.

Figure 4 Experimental time-domain responses. (a) With one buried object (*X*-band response). (b) With one buried object (*Ku*-band response). (c) With two buried objects (*Ku*-band response). ------ response at test point *P*1, ——— response at points *P*2 and *P*3

REFERENCES

1. T.P. Montoya and G.S. Smith, Land mine detection using a ground-penetrating radar based on resistively loaded vee dipoles, IEEE Trans Antennas Propagat 47 (1999), 1795−1806.
2. K. Demarest, R. Plumb, and Z. Huang, FDTD modeling of scatterers in stratified media, IEEE Trans Antennas Propagat 43 (1995), 1164−1168.
3. K.S. Yee, Numerical solution of initial boundary value problems involving Maxwell's equations in isotropic media, IEEE Trans Antennas Propagat AP-14 (1966), 302−307.
4. R. Luebbers, F.P. Hunsberger, K.S. Kunz, R.B. Standler, and M. Schneider, A frequency-dependent finite-difference time-domain formulation for dispersive materials, IEEE Trans Electromag Compat 32 (1990), 222−227.
5. G. Mur, Absorbing boundary conditions for the finite-difference approximation of the time-domain electromagnetic-field equations, IEEE Trans Electromag Compat EMC-23 (1981), 377−382.

© 2001 John Wiley & Sons, Inc.

FAR-FIELD PATTERN CALCULATION IN BODY-OF-REVOLUTION FINITE-DIFFERENCE TIME-DOMAIN (BOR – FDTD) METHOD

Wenhua Yu,[1] Nader Farahat,[1] and Raj Mittra[1]
[1] Electromagnetic Communication Laboratory
The Pennsylvania State University
University Park, Pennsylvania 16802

ABSTRACT: *In this paper, we present a far-field pattern calculation technique in the body-of-revolution finite-difference time-domain (BOR−FDTD) method. Because the BOR−FDTD solves two- and half-dimensional problems, it has different features from the three-dimensional FDTD method in the far-field pattern calculation. A monopole antenna fed by a coax is used to validate the technique described in this paper.* © 2001 John Wiley & Sons, Inc. Microwave Opt Technol Lett 31: 47−50, 2001.

I. INTRODUCTION

The numerical techniques based on the finite-difference time-domain (FDTD) algorithm applicable to general electromagnetic problems have grown in importance [1−5]. The BOR−FDTD has a great advantage over the three-dimensional FDTD for a rotationally symmetric problem [6−11]. It is well known that the three-dimensional near- to far-field transformation technique has been widely used to compute the far-field pattern in the FDTD simulations [4, 5]. Because